Journal of Photochemistry, 2 (1973/74) 409–420

VIOLET AND RED EMISSION BANDS OF THE CN RADICALS FORMED IN THE COLLISION OF METASTABLE ARGON ATOMS WITH CYANIDES

TSUNEO URISU* and KOZO KUCHITSU

Department of Chemistry, Faculty of Science, University of Tokyo, Bunkyo-ku, Tokyo (Japan)

(Received June 4, 1973)

SUMMARY

Violet and red emission spectra of CN formed in the dissociative excitation collision between metastable argon ($^3P_{0,2}$) atoms and HCN, CH_3CN, $(CN)_2$, ClCN and BrCN were observed in a flowing afterglow apparatus. The violet (0,0) sequences from HCN and CH_3CN showed a monotonic decrease in intensity with the vibrational quantum number up to $v=14$, whereas anomalous intensity enhancements of the (0,0), (5,5), (12,12) and (14,14) bands were observed for $(CN)_2$, ClCN and BrCN, in good agreement with a recent high-resolution study of Coxon, Setser and Duewer. With reference to the previous studies of Broida *et al.* and of Setser *et al.*, this difference in the vibrational populations is discussed in terms of the mechanism of formation of $CN(B^2\Sigma)$: In the HCN and CH_3CN cases a major fraction of the $CN(B^2\Sigma)$ radicals are produced directly by dissociative excitation. In the BrCN and ClCN cases, however, significant contributions to the populations of the $v = 0$, 5, 12 and 14 levels are also obtained due to their mixed $B^2\Sigma$–$A^2\Pi$ character from rotational perturbations. By the use of the known vibrational levels of $v = 12$ and 14 of the $B^2\Sigma$ state, the vibrational levels of $30 \geqslant v \geqslant 24$ of the $A^2\Pi$ state are estimated.

INTRODUCTION

The violet and red emissions of the CN radical are observed[1–5] by mixing cyanides into the afterglow of discharged argon gas. These emissions are ascribed to the dissociative excitation collision of metastable argon atoms with the cyanides:

$$Ar(^3P_{0,2}) + RCN \rightarrow Ar + R + CN\ (B^2\Sigma, A^2\Pi)$$
$$CN\ (B^2\Sigma) \rightarrow CN\ (X^2\Sigma) \quad \text{violet bands}$$
$$CN\ (A^2\Pi) \rightarrow CN\ (X^2\Sigma) \quad \text{red bands}$$

*Present address: Electrical Communication Laboratories, Nippon Telegraph and Telephone Public Corporation, Musashino-shi, Tokyo (Japan).

The violet and red emissions of the CN radical are also observed[6-12] in the reaction of active nitrogen with many organic compounds. In this case, a number of anomalies appear in the violet emission: exclusive enhancements of some rotational lines in addition to the appearance of extra lines in the (0,0) and (13,13) bands and a large spin splitting with unequal intensities in the (10,10) band[9]. From detailed studies of rotational structure of the (0,0) band and the pressure dependence of their intensities[7,8] the anomalies in the (0,0) band are due to the presence of rotational perturbation between the $B^2\Sigma$, $v=0$ and $A^2\Pi$, $v=10$ levels; most of the CN radicals are formed in the $A^2\Pi$ state, and the perturbed $B^2\Sigma$ levels are populated through their $A^2\Pi$ character.

The present work was undertaken to observe the violet and red emission spectra in the reaction of the metastable argon with five CN-containing compounds. When our measurements were nearly completed and the present manuscript was in preparation, Professor D. W. Setser and co-workers informed us of their recent paper[13], in which they reported a detailed study of the violet and red systems of CN in emission, from the reactions of $Xe(^3P_2)$ and $Ar(^3P_{0,2})$ with HCN, BrCN and ICN. The $B^2\Sigma$–$X^2\Pi$ system was observed at high resolution and several new rotational perturbations were found. Our present observations are in good agreement with theirs.

EXPERIMENTAL

The flowing afterglow apparatus described elsewhere[4] was used in the present experiment. Metastable argon atoms were produced by a 2450 MHz microwave discharge through argon at an input power of about 0.5 kW.

The cyanide gas was admixed 15 cm downstream from the discharge region. The pressure was measured by a Pirani gauge calibrated by a McLeod gauge. The pressure of argon and the cyanide were 0.2–0.9 Torr and about 0.02 Torr, respectively. Most spectroscopic observations were made with the argon gas pressure of 0.3 Torr. At this pressure the vibrational relaxation times are assumed to be sufficiently long in comparison with the radiative lifetime of $CN(B^2\Sigma)$, 85 ns[6,15], and the vibrational relaxation in the $B^2\Sigma$ state is ignored.

The spectra were observed by use of a 0.5 m Czerny–Turner scanning monochromator with a scanning speed of 70 Å/min and a time constant of 3 s. A slit width of 140 μm resulted in the resolution of about 3 Å. Mechanically chopped luminescences were detected by a photomultiplier and a lock-in amplifier. A relative intensity calibration for the monochromator photomultiplier combination was made using a halogen lamp. Argon, BrCN and CH_3CN were obtained commercially and used without further purification. HCN and ClCN were prepared[16] by the reaction of NaCN with sulfuric acid and with chlorine, respectively, and cyanogen was prepared[16] by the thermal decomposition of AgCN. No impurity effect was observed in any of the present measurements.

The presence of argon metastable species in the discharged flow was confirmed by observation of the nitrogen second positive band system ($C^3\Pi$–$B^3\Pi$). When nitrogen gas of about 0.05 Torr was introduced into the argon afterglow, a strong N_2 second positive band from the vibrational levels $v \leqslant 2$ was observed. According to previous studies[17,18], this spectrum is characteristic of the collision of N_2 with metastable argon ($^3P_{0,2}$) atoms. Wavelength calibration was obtained by reference to the emission lines of a mercury lamp.

OBSERVED SPECTRA

The discharged argon stream was non-luminous in the flow tube. When cyanide was mixed into this stream through an inlet nozzle of 0.4 mm i.d. stainless-steel tube, a cone-shaped diffusion flame appeared on top of the inlet nozzle. The color of this flame was a mixture of blue white and russet. The brightness of the flame changed significantly with the argon pressure and the power of discharge. Sequences of bands with $\Delta v = -1$ and 0 of the violet system were sufficiently intense for convenient observation in the present analysis. The red system was also observed for all the cyanides, and their spectra were recorded between 5700 and 6900 Å. The red bands are expected at wavelengths longer than 6900 Å, outside the range of the present observations.

The microwave discharge was pulsed at 100 Hz pulse, and the delay time between the discharge pulse and the emission pulse in the reaction zone was measured. The delay time was approximately equal to the flight time of the argon atom from the discharge section to the reaction zone. From this observation, it was confirmed that any direct u.v. photolysis by the discharge was negligible. Band assignments were made according to the table by Wallace[19]. The assignments of the enhanced rotational lines given in the following discussion were confirmed by the high-resolution spectrum of the violet band reported by Coxon *et al.*[13] in the reaction of metastable argon with BrCN.

The intensities of the violet and red emissions from all the cyanides studied and that of the second positive emission of nitrogen had similar dependence on the argon pressure. The intensities first increased nearly linearly with the argon pressure and then started to decrease, as illustrated in Fig. 4 of ref. 4 for CH_3CN and HCN.

HCN

Figure 1 (a) shows the (0,0) and (0,1) sequences of the violet emission spectrum from the reaction of metastable argon ($^3P_{0,2}$) atoms with HCN. The relative intensity distribution of the vibrational structure of the $\Delta v = 0$ sequence decreases from the (0,0) to the (14,14) bands. The vibrational structure is observed only up to (14,14) in agreement with earlier work[1,13, 20–22]. In the argon pressure range of 0.2–0.6 Torr, no significant change is observed in the relative intensity distribution

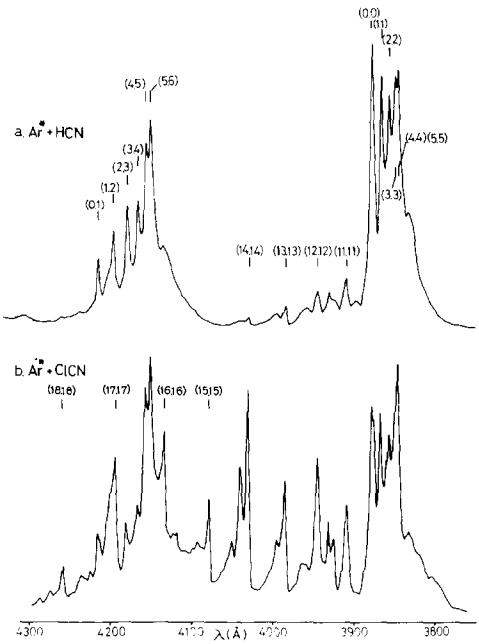

Fig. 1. Violet emission spectra of (a) Ar* + HCN and (b) Ar* + ClCN. The pressures of argon and cyanide gases are 0.3 and about 0.02 Torr, respectively.

of the spectrum. At the argon pressure of above 0.7 Torr, however, the vibrational bands (15,15)–(18,18) and a weak CH (4315 Å) band were detected, and the intensities of these bands relative to the (0,0)–(14,14) bands increased as the argon pressure was increased. This might indicate a contribution from a mechanism other than a single collision between metastable argon with HCN to the production of $CN(B^2\Sigma)$ in this high-pressure range. No systematic experiment has been made, however, to further study the reaction mechanism in this condition.

The emission spectrum of the red bands, shown in Fig. 2, has an intensity maximum at $v' = 6$–8, and the relative intensity distribution of the vibrational structure shows no significant change in the argon pressure from 0.2 to 0.9 Torr.

CH_3CN

In the CH_3CN case, the intensity distribution of the vibrational structure of the violet bands shows a monotonic decrease[4] from (0,0) to (14,14) similar to that from HCN. However, the excitation to higher vibrational levels is much weaker than that in the HCN case. On the other hand, the red band from CH_3CN has nearly the same intensity profile as that from HCN. At an argon pressure higher than 0.2 Torr, the CH (4315 Å) band appears. The intensity of this band, in contrast to the violet and red bands, increases steeply beyond about 0.4 Torr[4], indicating that the mechanism of formation of $CH(A^2\Delta)$ is different from that of CN ($B^2\Sigma$ and $A^2\Pi$).

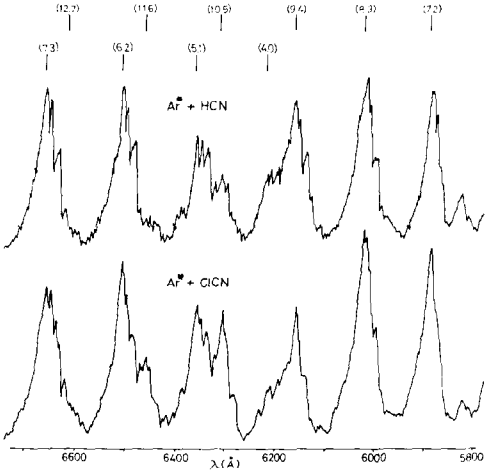

Fig. 2. Red emission spectra of Ar* + HCN and Ar* + ClCN. The pressures of argon and cyanide gases are 0.3 and about 0.02 Torr, respectively.

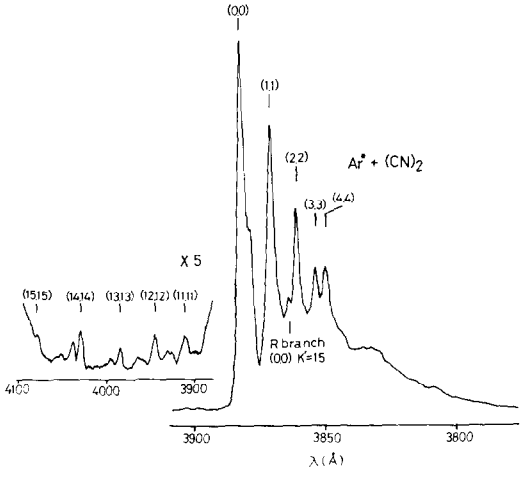

Fig. 3. Violet emission spectrum of Ar* + $(CN)_2$. The slit widths of the spectrum are 140 and 200 μm for the lower and upper traces, respectively.

$(CN)_2$

The violet bands from $(CN)_2$ (Fig. 3) also show a nearly monotonic decrease, and higher vibrational levels are observed up to $v' = 15$ with intensities weaker than the corresponding transitions from CH_3CN. However, a deviation from a uniform trend is observed in the appearance of a small peak at 3864.5 Å and in the slight enhancements of the (12,12) and (14,14) bands, which are not observed in the HCN and CH_3CN cases. The peak at 3864.5 Å is known to be the enhanced $K' = 15$ rotational line of the (0,0) band[13]. The red bands from $(CN)_2$ have an intensity profile similar to those from HCN and CH_3CN.

ClCN and BrCN

For ClCN the violet emission band has strong excitation of higher vibrational levels ($v' \geqslant 11$) of the $B^2\Sigma$ state, as shown in Fig. 1 (b) with assignments up to (18,18). The intensity distribution of the vibrational structure shows a significant deviation from a monotonic decrease, unlike those from HCN, CH_3CN and $(CN)_2$. Intensity enhancements are observed in the (0,0), (5,5), (12,12) and (14,14) bands, whereas the (2,2) and (3,3) bands are weaker than those from HCN and CH_3CN. The enhanced rotational line $K' = 15$ of the (0,0) band, which appears in the $(CN)_2$ case, is also observed as a shoulder of the (2,2) band. The intensity distribution of the vibrational structure shows no significant change as the argon pressure is varied from 0.2 to 0.9 Torr.

For BrCN the profile of the violet emission spectrum is similar to that from ClCN. However, the excitation to higher vibrational levels, the fluctuations in the vibrational intensity distribution and the enhancement of the rotational line $K' = 15$ of the (0,0) band are more prominent than for ClCN. The intensity distribution of the vibrational structure shows no significant change as the argon pressure is varied from 0.2 to 0.6 Torr, except for the (11,11) band, where the intensity relative to the other bands decreases as the argon pressure is increased, as observed by Coxon *et al.*[13]. This tendency is also observed in the (11,11) band from ClCN.

Qualitative features of the red bands from ClCN (Fig. 2) and BrCN are similar to those from the other cyanides except for the relatively strong excitations to higher vibrational levels, as demonstrated in the appearance of the (11,6) and (12,7) bands in the red bands from ClCN and BrCN.

Relative intensities of the red emissions to the violet emissions

The color of the emission flame is slightly different from one cyanide to another. This difference is considered to be due to the fact that the intensity ratio of the red emission to the violet emission is different among the cyanides. The relative intensities of the red band (10,5) to the violet band (0,0) observed with the argon pressure of 0.2 Torr are shown in Table 1. For comparison, the nature of

TABLE 1

RELATIVE INTENSITIES OF RED AND VIOLET BANDS AND INTENSITY DISORDER

Parent molecule	$I(R)/I(V)$[a]	Intensity distribution of the violet band
HCN	1	monotonic decrease
CH_3CN	1	(0,0) → (14,14)
$(CN)_2$	2.4	weak disorder
ClCN	4.7	strong disorder
BrCN	5.3	

[a] Intensity ratio of the red band (10,5) to the violet band (0,0) normalized to that from HCN.

the intensity distribution of the violet emission spectrum is also given in Table 1. The relative intensity of the red band increases in the order: HCN $\approx$ CH_3CN < $(CN)_2$ < ClCN < BrCN.

VIBRATIONAL POPULATIONS OF CN($B^2\Sigma$)

The observed relative intensities of the violet bands (v',v'') were reduced to the relative vibrational populations $N_{v'}$ of the $B^2\Sigma$ state by use of the following equation[23]:

$$I_{v'v''} = \text{const. } N_{v'} \nu_{v'v''}^4 q_{v'v''} , \quad (1)$$

where $\nu_{v'v''}$ and $q_{v'v''}$ are the wavenumber and the Franck–Condon factor of the transition (v',v''), respectively. Spindler's table[24] of the Franck–Condon factors was used for the calculation.

The vibrational population distribution was estimated mainly by use of the $\Delta v = 0$ sequence. However, since the (0,0)–(10,10) bands are strongly overlapped, the populations of the $v' = 0$, 1, 2 and 3 levels were estimated from the $\Delta v = 0$ and -1 sequences. For HCN, CH_3CN and $(CN)_2$ (Fig. 4) the populations estimated by use of eqn. (1) were refined by a calculation of band envelopes[5]. For BrCN and ClCN, however, only partial and approximate estimates (Fig. 5) were possible

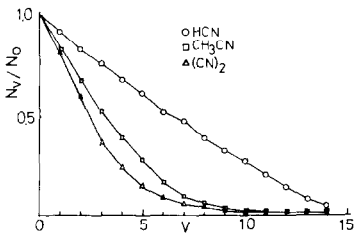

Fig. 4. Relative vibrational populations of the CN($B^2\Sigma$) radicals produced by the reactions of Ar* + HCN, Ar* + CH_3CN and Ar* + $(CN)_2$. The pressures of argon and cyanide gases are 0.3 and about 0.02 Torr, respectively.

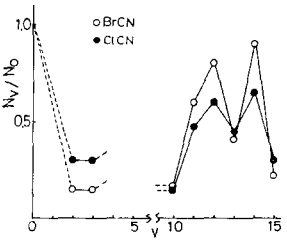

Fig. 5. Relative vibrational populations of CN($B^2\Sigma$) produced by the reactions of Ar* + BrCN and Ar* + ClCN. The pressures of argon and cyanide gases are 0.3 and about 0.02 Torr, respectively.

because of the overlapping of the spectra. Nevertheless, they are adequate for the following qualitative discussion. The monotonic decrease towards higher vibrational levels of the population curves is more rapid for CH_3CN and $(CN)_2$ than that for HCN (Fig. 4). This difference is accounted for by the following reasoning. The available energy for excitation (the difference between the energy of the metastable argon atom and the dissociation energy of the cyanide) is nearly equal (about 6.3 eV) for the three cyanides. In the case of CH_3CN and $(CN)_2$, however, a significant fraction of this energy can be transmitted to the internal energies of the CH_3 and CN radicals. Excitation to higher vibrational levels is less probable.

The degree of disorder in the population distribution is larger for BrCN than for ClCN. Population maxima are observed at $v' = 0$, 12 and 14 for BrCN and ClCN, and a similar trend is observed in the spectrum for $(CN)_2$ shown in Fig. 3. This contrasts with the reaction of active nitrogen and organic compounds[9], where the population maxima in the $B^2\Sigma$ state are observed at $v' = 0$ and 5. Although the population of the $v' = 5$ level could not be estimated in the present work because of the excessive overlapping with other bands, the violet bands for ClCN and BrCN show intense peaks at the position of the (5,5) band. With this result and the discussion in the following section, it is probable that these peaks are mainly composed of the (5,5) band and that another population maximum exists at $v' = 5$ for these cyanides.

FORMATION MECHANISM OF CN($B^2\Sigma$)

Certain rotational levels of the $B^2\Sigma$ state are located so close to the rotational levels of the $A^2\Pi$ state with the same J values that they perturb each other. Since the wave-functions of the $B^2\Sigma$ state are mixed with those of the $A^2\Pi$ state as a result of this perturbation, two mechanisms can produce the CN($B^2\Sigma$) radical[8,9]: (1) direct formation of the $B^2\Sigma$ state; and (2) production of $B^2\Sigma$ through its $A^2\Pi$ character due to the rotational perturbation.

The violet emission spectrum should reveal the formation mechanism. If the $B^2\Sigma$ state is produced exclusively through the process (2), the rotational lines from the perturbed levels alone should be observed at a low pressure. In the present work, where the rotational structure of the spectra is not resolved, this effect appears as an enhancement of certain vibrational bands.

The perturbed levels are described[7] by the wavefunctions:

$$\psi^{A} = (1-\varrho^2)^{1/2}\psi_a - \varrho^*\psi_b \quad (2)$$

and

$$\psi^{B} = \varrho\psi_a + (1-\varrho^2)^{1/2}\psi_b \quad (3)$$

where ψ_a and ψ_b are the unperturbed wavefunctions of the $A^2\Pi$ and $B^2\Sigma$ states, respectively, and ϱ is the degree of mixing of the two levels. When the B state is produced through the process (2), strong emissions should be observed only from the perturbed levels with large ϱ, which depends on the unperturbed energy

separation δ and the perturbation matrix element S. Since S is proportional to the overlap integral of the vibrational wavefunctions, $\int \psi_v^* \psi_{v'} dr$, of the two perturbed levels, S is considered to make a slowly-varying contribution to the disorder of the intensity distribution. On the other hand, the energy interval δ can be as small as 1 cm^{-1} because of the accidental degeneracy between the rotational levels of the B and A states with the same J values, and ϱ can be so large as to cause a significant disorder in the intensity distribution. The condition for this degeneracy is expressed, neglecting centrifugal distortion, as:

$$U_A(v_A) + B_{A,v}J(J+1) = U_B(v_B) + B_{B,v}J(J+1) \tag{4}$$

where $U(v)$ and B_v are the energy and the rotational constant of vibrational level v. When the CN($B^2\Sigma$) radical is produced through process (2), strong emission of $B^2\Sigma$ appears from those perturbed levels where the corresponding perturbed levels of $A^2\Pi$ are sufficiently populated. This implies that eqn. (4) has to be satisfied at relatively low J levels, say $J \lesssim 20$, and that:

$$[U_A(v_A) - U_B(v_B)]/(B_{B,v} - B_{A,v}) = J(J+1) \lesssim 500 \tag{5}$$

Since $B_{B,0} - B_{A,0} \approx 0.4$ cm^{-1} [19], the energy separation between the A and B vibrational levels must lie in the range:

$$0 < [U_A(v_A) - U_B(v_B)] \lesssim 200 \text{ cm}^{-1} \approx 0.025 \text{ eV} \tag{6}$$

According to the present observations, the population maxima observed in the $v = 0$, 5, 12 and 14 levels of $B^2\Sigma$ from BrCN and ClCN should meet this requirement.

The vibrational levels, $v_B = 0$, 5 and 10, of the $B^2\Sigma$ state are nearly degenerate with the $v_A = 10$, 17 and 24 levels of the $A^2\Pi_{3/2}$ state, respectively, within 0.01 eV, as shown in Fig. 6*[19,22]. The $^2\Pi_{3/2}$ spin orbit components lie approximately 50 cm^{-1} higher than $^2\Pi_{3/4}$. For a discussion of the vibrational levels above $v_A = 24$, however, these states are not distinguished. The two components are collectively labelled $A^2\Pi_i$, since the uncertainty of about 80 cm^{-1} in the following estimate of their energies is larger than the spin–orbit splitting.

The energies $U(v)$ of the vibrational levels above $v = 24$ in the $A^2\Pi_i$ state can be extrapolated by use of the third-order equation:

$$U(v) = a + bv + cv^2 + dv^3 \tag{7}$$

where the coefficients are determined by the known $U(v)$ values at $v_A = 21$, 22, 23 and 24. From the estimated energies, the $v_A = 27$ and 30 levels of the $A^2\Pi_i$ state are shown to be nearly degenerate with the $v_B = 12$ and 14 levels of the $B^2\Sigma$ state, respectively.

* The vibrational energy levels up to $v = 18$ of the $B^2\Sigma$ and $A^2\Pi$ states are given in ref. 22. The energies of the $A^2\Pi$ vibrational levels for $v = 19$ to 24 are obtained from the Q_1 band head positions presented in ref. 19.

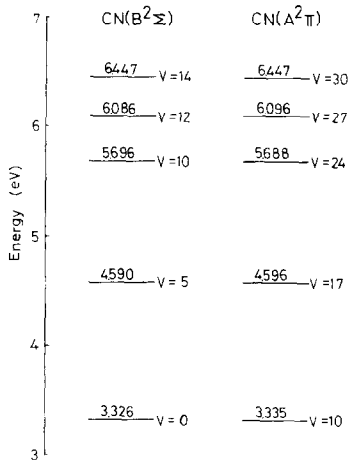

Fig. 6. Energies of the vibrational levels of the $B^2\Sigma$ and $A^2\Pi$ states. Only nearly degenerate levels are shown. The observed vibrational levels for $v_A \leqslant 24$ refer to those of the $A^2\Pi_{3/2}$ state. For the estimated levels, $v_A > 24$, no distinction between the $A^2\Pi_{3/2}$ and $A^2\Pi_{1/2}$ states can be made. See text and Table 2.

As for the $v_B = 10$ levels of the $B^2\Sigma$ state, the condition (6) is not satisfied, even though it is nearly degenerate with the $v_A = 24$ level of the $A^2\Pi_{3/2}$ state (Fig. 6), since $U_A(24) - U_B(10)$ is negative (about −0.009 eV). Only weak rotational perturbations can exist in any of the J levels. This prediction is given experimental support by the high-resolution spectrum of the violet (10,10) band observed by Brown and Broida[9] who reported a series of spin splittings with unequal intensities appearing in all the rotational transitions in a uniform manner. In the strong rotational perturbations existing in the $v_B = 0$, 5, 12 and 14 levels, unperturbed energy differences δ between $B^2\Sigma$ and one of $A^2\Pi_{3/2}$ or $A^2\Pi_{1/2}$ are smaller than 1 cm^{-1} for particular J values, so that a contribution from the other component of the $A^2\Pi$ state to the perturbation can be disregarded. In the (10,10) band, however, since the unperturbed energy separations are about 72 and 22 cm^{-1} for the $B^2\Sigma$–$A^2\Pi_{3/2}$ and $B^2\Sigma$–$A^2\Pi_{1/2}$ perturbations, respectively, the perturbation matrix has to be solved for the three levels. Another characteristic of the rotational perturbation in the (10,10) band is that the spin splitting is large ($\sim$ 1 cm^{-1}) whereas δ is large, and that the intensity enhancement is weak in comparison with the perturbations in other levels[9]. A simple estimate following the arguments in refs. 8 and 9 suggests that the overlap integral of the vibrational wavefunctions for $v_B = 10$ and $v_A = 24$ is about an order of magnitude larger than that for $v_B = 0$ and $v_A = 10$.

The above consideration on the population maxima observed in the BrCN and ClCN cases provides evidence for the fact that the strong B–A rotational perturbation exists in these levels and that most of the $CN(B^2\Sigma)$ radicals are produced through the mechanism (2) in these cases. On the other hand, since no significant population disorder is observed in the HCN and CH_3CN cases, a major

fraction of the CN($B^2\Sigma$) radicals are produced through the mechanism (1). Excitation with cyanogen seems to be an intermediate case.

The above argument is further supported by the observed relative intensity of the red band to the violet bands. Population of the $A^2\Pi$ state relative to $B^2\Sigma^+$ should increase as the relative importance of the process (2) increases. As shown in Table 1, the observed relative intensities increase according to the degrees of disorder in the intensity distribution of the violet emission band.

As mentioned in the preceding section, the relative intensity of the violet (11,11) band shows a pressure dependence different from the other bands for BrCN and ClCN. This agrees with the finding of Coxon *et al.*[3,13] that a perturbation by a state other than $A^2\Pi$ exists in the $v_B = 11$ level of the $B^2\Sigma$ state.

VIBRATIONAL ENERGY LEVELS OF CN($A^2\Pi$) ABOVE $v = 24$

The vibrational energy levels of the $A^2\Pi$ state have been observed[19] spectroscopically only up to $v_A = 24$. Since the above arguments indicate that $v_B = 14$ of $B^2\Sigma$ and $v_A = 30$ of $A^2\Pi_i$ are nearly degenerate, the potential energy of the $v_A = 30$ level of $A^2\Pi_i$ is estimated to be 6.447 ± 0.010 eV from the known potential energy[22] of the $v_B = 14$ level. The coefficients of eqn. (7) were determined so as to reproduce the energies of the $v_A = 22$, 23, 24 and 30 levels: $a = 2.273$ eV, $b = 8.418 \times 10^{-2}$ eV, $c = 4.779 \times 10^{-3}$ eV and $d = -9.825 \times 10^{-5}$ eV. The calculated potential energies for the $v_A = 20$–30 levels are listed in Table 2.

ACKNOWLEDGEMENTS

The authors are indebted to Professor D. W. Setser of Kansas State University for informing them of his recent experimental results before publication and for helpful comments. Thanks are also due to research grants from the Ministry of Education of Japan and Takeda Science Foundation.

TABLE 2

POTENTIAL ENERGIES (eV) OF THE VIBRATIONAL LEVELS OF CN ($A^2\Pi$)

v	obs.[a]	calc.[b]	v	obs.[a]	calc.[b]
20	5.082	5.082	26	—	5.966
21	5.238	5.238	27	(6.086)[c]	6.096
22	5.392	(5.392)	28	—	6.220
23	5.542	(5.542)	29	—	6.337
24	5.688	(5.688)	30	(6.447)[d]	(6.447)
25	—	5.829			

[a] Estimated from spectroscopic data given in ref. 19.

[b] Calculated by eqn. (7) with parameters derived from the observed energies for $v = 22$, 23, 24 and 30. See text.

[c,d] Assumed to be equal to the potential energies of the $v = 12$ and 14 levels of the $B^2\Sigma$ state, respectively, given in ref. 22.

REFERENCES

1 D. W. Setser and D. H. Stedman, *J. Chem. Phys.*, 49 (1968) 467.
2 D. H. Stedman and D. W. Setser, *Progress in Reaction Kinetics*, Vol. 6, Part 4, Pergamon, Oxford, 1971.
3 W. H. Duewer, J. A. Coxon and D. W. Setser, *J. Chem. Phys.*, 56 (1972) 4355.
4 T. Urisu and K. Kuchitsu, *Chem. Lett.*, (1972) 813.
5 T. Urisu and K. Kuchitsu, *Chem. Phys. Lett.*, 18 (1973) 337.
6 K. D. Bayes, *Can. J. Chem.*, 39 (1961) 1074.
7 H. E. Radford and H. P. Broida, *Phys. Rev.*, 128 (1962) 231.
8 H. E. Radford and H. P. Broida, *J. Chem. Phys.*, 38 (1963) 644.
9 R. L. Brown and H. P. Broida, *J. Chem. Phys.*, 41 (1964) 2053.
10 T. Iwai, D. W. Pratt and H. P. Broida, *J. Chem. Phys.*, 49 (1968) 919.
11 T. Iwai, M. I. Savadatti and H. P. Broida, *J. Chem. Phys.*, 47 (1967) 3861.
12 G. M. Provencher and D. J. McKenney, *Can. J. Chem.*, 50 (1972) 2527.
13 J. A. Coxon, D. W. Setser and W. H. Duewer, *J. Chem. Phys.*, 58 (1973) 2244.
14 R. G. Bennett and F. W. Dalby, *J. Chem. Phys.*, 36 (1962) 399. A smaller value (τ = 39.4 ns) was estimated recently in ref. 15.
15 T. J. Cook and D. H. Levy, *J. Chem. Phys.*, 57 (1972) 5059.
16 G. Brauer, *Handbook of Preparative Inorganic Chemistry*, Vol. I, Academic Press, New York, 1963.
17 E. S. Fishburne, *J. Chem. Phys.*, 47 (1967) 58.
18 D. W. Setser, D. H. Stedman and J. A. Coxon, *J. Chem. Phys.*, 53 (1970) 1004.
19 L. Wallace, *Astrophys. J. (Suppl. Ser.)*, 7 (1962) 165.
20 C. E. Moore (ed.), Nat. Bur. Stand. Circ. No. 467 *Atomic Energy Levels*, U.S. Dept. Commerce, Washington, D.C., 1962, as cited in ref. 2.
21 D. D. Davis and H. Okabe, *J. Chem. Phys.*, 49 (1968) 5526.
22 R. J. Fallon, J. T. Vanderslice and R. D. Chloney, *J. Chem. Phys.*, 37 (1962) 1097.
23 G. Herzberg, *Molecular Spectra and Molecular Structure*, Vol. I, Van Nostrand, New York, 1950.
24 R. J. Spindler, *J. Quant. Spectros. Radiat. Transf.*, 5 (1965) 165.